

Interaction of inhomogeneous axions with magnetic fields in the early universe

Maxim Dvornikov*

Pushkov Institute of Terrestrial Magnetism, Ionosphere
and Radiowave Propagation (IZMIRAN),
108840 Moscow, Troitsk, Russia

Abstract

We study the system of interacting axions and magnetic fields in the early universe after the quantum chromodynamics phase transition, when axions acquire masses. Both axions and magnetic fields are supposed to be spatially inhomogeneous. We derive the equations for the spatial spectra of these fields, which depend on conformal time. In case of the magnetic field, we deal with the spectra of the energy density and the magnetic helicity density. The evolution equations are obtained in the closed form within the mean field approximation. We choose the parameters of the system and the initial condition which correspond to realistic primordial magnetic fields and axions. The system of equations for the spectra is solved numerically. We study the evolution of the fields for different seed spectra of axions. We find that the mutual interaction between axions and magnetic fields is suppressed for the chosen realistic parameters of the system, that is in agreement with previous results where only the zero mode of axions was accounted for.

1 Introduction

The existence of axions, which are pseudoscalar particles, was theoretically proposed in Ref. [1] to provide the conservation of the CP symmetry in the quantum chromodynamics (QCD). The conserved CP symmetry is required, in particular, because of the experimental non-observation of an electric dipole moment of a neutron (see, e.g., Ref. [2]). There are numerous studies of the models for QCD axions which are summarized in Ref. [3].

Currently, there are active searches for axions in laboratory experiments. These particles can be probed in their interactions with electromagnetic fields, fermion spins, and nuclear electric dipole moments. The difficulty of the direct axion observation is because of the smallness of corresponding coupling constants. Major present experimental studies of axions are reviewed in Ref. [4]. There are recent claims (see, e.g., Ref. [5]) that some experimental data can be interpreted as the axions observation. However, more careful studies to confirm such findings are required.

Besides laboratory studies, there are attempts to detect axions from astrophysical sources and cosmological media. One can try to capture axions produced in the Sun using existing and future helioscopes (see, e.g., Ref. [6]). Additionally, axions produced in neutron stars can result in their X-ray emission [7], which is observed by satellite based telescopes. Axions,

*maxdvo@izmiran.ru

which the cold dark matter halo in our Galaxy consists of, can be detected using a haloscope technique. There are many haloscopes techniques, which are described in Ref. [8].

The interest to the experimental study of astrophysical and cosmological axions is motivated by the fact that these particles can both solve the CP symmetry problem in QCD and be one of the most plausible candidate for the dark matter [9]. There are numerous sources of axions in the early universe. These particles can be produced in decays of more massive particles or topological defects, be thermally emitted by other constituents of the standard model etc. Some of these mechanisms are reviewed in Ref. [10].

Cosmological axions are believed to be spatially homogeneous. However, if the Peccei-Quinn phase transition, which takes place at $T_{\text{PQ}} \approx f_a = (10^{10} - 10^{12}) \text{ GeV}$, where f_a is the Peccei-Quinn constant, happens after the reheating during the inflation, then nonzero spatial modes of axions can appear. Such a scenario is also not excluded (see, e.g., Refs. [9, 10]). Inhomogeneous axions were proposed in Ref. [11] to result in the formation of Bose stars. The evolution of axion miniclusters was recently studied in Ref. [12].

In the present work, we study the evolution of the system of cosmological axions and magnetic fields. For the first time, analogous problem was considered in Ref. [13]. However, nontrivial spectra of neither axions nor a magnetic field were considered in Ref. [13]. Moreover, the universe expansion was not accounted for properly there. In Ref. [14], we refined the analysis of Ref. [13] by considering the spectral distribution of a primordial magnetic field and taking into account the time dependent scale factor $a \neq 1$. Now, we generalize the results of Ref. [14] by accounting for an arbitrary spatial spectrum of axions.

As mentioned in Refs. [13, 14], a magnetic field in the presence of an axion can be unstable. Indeed, in this case, the induction equation gets the contribution, $\propto (\nabla \times \mathbf{B})$, analogous to that for the chiral magnetic effect (the CME) [15]. The axion wavefunction contributes to the α -dynamo parameter responsible for the magnetic field instability. Thus, the consideration of inhomogeneous axions is equivalent to the study of chiral media with a coordinate dependent chiral imbalance. This problem was studied in Ref. [16]. However, unlike the CME case with a coordinate dependent chiral imbalance, here, we have a well established wave equation for the axion wavefunction interacting with an electromagnetic field.

Our work is organized in the following way. In Sec. 2, we derive the general equations for the spectra of the magnetic energy and helicity densities in the presence of an inhomogeneous axion. The equation for the Fourier transform of the axion wavefunction was considered in Sec. 3. Applying the mean field approximation, we combine the obtained equations to the closed system in Sec. 4. In Sec. 5, we choose parameters in the system, corresponding to the realistic cosmological medium, and define the initial condition. We present the results of the numerical simulations in Sec. 6. Finally, we conclude in Sec. 7.

2 Magnetic field in the presence of inhomogeneous axions

The equations for the electromagnetic field $F_{\mu\nu}$, interacting with a scalar axion field φ , in curved spacetime with the coordinates $x^\mu = (t, \mathbf{x})$ read

$$\begin{aligned} \frac{1}{\sqrt{-g}} \partial_\nu (\sqrt{-g} F^{\mu\nu}) + g_{\alpha\gamma} \partial_\nu \varphi \tilde{F}^{\mu\nu} + J^\mu &= 0, \\ \frac{1}{\sqrt{-g}} \partial_\nu (\sqrt{-g} \tilde{F}^{\mu\nu}) &= 0, \end{aligned} \tag{2.1}$$

where $\tilde{F}^{\mu\nu} = \frac{1}{2}E^{\mu\nu\alpha\beta}F_{\alpha\beta}$ is the dual counterpart of $F_{\mu\nu}$, $E^{\mu\nu\alpha\beta} = \frac{1}{\sqrt{-g}}\varepsilon^{\mu\nu\alpha\beta}$ is the covariant antisymmetric tensor, $\varepsilon^{0123} = +1$, $g = \det(g_{\mu\nu})$, $g_{\mu\nu}$ is the metric tensor, $g_{a\gamma}$ is the coupling constant, and $J^\mu = (\rho, \mathbf{J}/a)$ is the external current. We consider the Friedmann-Robertson-Walker (FRW) metric $g_{\mu\nu} = \text{diag}(1, -a^2, -a^2, -a^2)$, where $a(t)$ is the scale factor. Using the conformal variables [17] $\mathbf{E}_c = a^2\mathbf{E}$, $\mathbf{B}_c = a^2\mathbf{B}$, $\rho_c = a^3\rho$, and $\mathbf{J}_c = a^3\mathbf{J}$, we rewrite Eq. (2.1) in the form,

$$(\nabla \times \mathbf{B}_c) = \mathbf{E}'_c + \mathbf{J}_c + g_{a\gamma}\varphi'\mathbf{B}_c + g_{a\gamma}(\nabla\varphi \times \mathbf{E}_c), \quad (2.2)$$

$$(\nabla \times \mathbf{E}_c) = -\mathbf{B}'_c, \quad (2.3)$$

$$(\nabla\mathbf{E}_c) = -g_{a\gamma}(\mathbf{B}_c\nabla)\varphi + \rho_c, \quad (2.4)$$

$$(\nabla\mathbf{B}_c) = 0, \quad (2.5)$$

where the prime means the derivative with respect to the conformal time η defined by $dt = a d\eta$.

Supposing that $\mathbf{J}_c = \sigma_c\mathbf{E}_c$, where $\sigma_c = 10^2$ is the conformal conductivity of ultrarelativistic plasma, and neglecting the displacement current \mathbf{E}'_c in Eq. (2.2), we get that the electric field has the form,

$$\mathbf{E}_c = \frac{1}{\sigma_c} [(\nabla \times \mathbf{B}_c) - g_{a\gamma}\varphi'\mathbf{B}_c] - \frac{1}{\sigma_c^2} [g_{a\gamma}(\nabla\varphi \times (\nabla \times \mathbf{B}_c)) + g_{a\gamma}^2\varphi'(\mathbf{B}_c \times \nabla\varphi)]. \quad (2.6)$$

Here we keep the terms linear in $\nabla\varphi$. Setting $\rho_c = 0$ in Eq. (2.4), we derive the equation for \mathbf{B}_c ,

$$\begin{aligned} \mathbf{B}'_c &= \frac{1}{\sigma_c} [\Delta\mathbf{B}_c + g_{a\gamma}\varphi'(\nabla \times \mathbf{B}_c) + g_{a\gamma}(\nabla\varphi' \times \mathbf{B}_c)] \\ &+ \frac{g_{a\gamma}}{\sigma_c^2} \{((\nabla \times \mathbf{B}_c) \cdot \nabla)\nabla\varphi - (\nabla\varphi \cdot \nabla)(\nabla \times \mathbf{B}_c) - (\nabla \times \mathbf{B}_c)\Delta\varphi\} \\ &+ \frac{g_{a\gamma}^2}{\sigma_c^2} \{\mathbf{B}_c [\varphi'\Delta\varphi + (\nabla\varphi' \cdot \nabla\varphi)] + \varphi' [(\nabla\varphi \cdot \nabla)\mathbf{B}_c - (\mathbf{B}_c \cdot \nabla)\nabla\varphi] - \nabla\varphi(\mathbf{B}_c \cdot \nabla)\varphi'\}, \end{aligned} \quad (2.7)$$

where we use Eqs. (2.3) and (2.6).

Equation (2.7) can be simplified if we assume that axions are inhomogeneous but isotropic. It means that, after the spatial averaging, one has that $\langle\nabla\varphi\rangle = 0$, whereas $\langle(\nabla\varphi)^2\rangle \neq 0$ and $\langle\Delta\varphi\rangle \neq 0$. Keeping the terms linear in $g_{a\gamma}$ in Eq. (2.7) and spatially averaging it, we get the modified induction equation,

$$\mathbf{B}'_c = \frac{1}{\sigma_c}\Delta\mathbf{B}_c + \alpha(\mathbf{x})(\nabla \times \mathbf{B}_c), \quad \alpha(\mathbf{x}) = \frac{g_{a\gamma}}{\sigma_c} \left(\varphi' - \frac{2}{3\sigma_c}\Delta\varphi \right), \quad (2.8)$$

where we omit the averaging brackets for the sake of brevity. In Eq. (2.8), the α -dynamo parameter $\alpha(\mathbf{x})$, which is the coefficient in the magnetic instability term $\propto (\nabla \times \mathbf{B}_c)$, is different from that in Refs [13, 14]. It gets the contribution from the inhomogeneous axion field $\propto \Delta\varphi$.

It is convenient to deal with a Fourier transform, which has the form, $f_{\mathbf{k}} = \int d^3x e^{i\mathbf{k}\mathbf{x}} f(\mathbf{x})$, and $f_{\mathbf{k}}^* = f_{-\mathbf{k}}$ since $f(\mathbf{x})$ is real. Then we define the spectra of the magnetic energy density

and the magnetic helicity,

$$\begin{aligned}\rho_{\mathbf{p}}(\eta) &= \frac{1}{2} \int d^3x e^{i\mathbf{p}\mathbf{x}} \mathbf{B}_c^2(\mathbf{x}) = \frac{1}{2} \int \frac{d^3k}{(2\pi)^3} (\mathbf{B}_{\mathbf{k}}^{(c)*} \mathbf{B}_{\mathbf{k}+\mathbf{p}}^{(c)}), \\ h_{\mathbf{p}}(\eta) &= \int d^3x e^{i\mathbf{p}\mathbf{x}} (\mathbf{A}_c(\mathbf{x}) \mathbf{B}_c(\mathbf{x})) = \int \frac{d^3k}{(2\pi)^3} (\mathbf{A}_{\mathbf{k}}^{(c)*} \mathbf{B}_{\mathbf{k}+\mathbf{p}}^{(c)}).\end{aligned}\quad (2.9)$$

Note that the total magnetic helicity,

$$H(\eta) = \int d^3x (\mathbf{A}_c \mathbf{B}_c) = \int \frac{d^3p}{(2\pi)^3} (\mathbf{A}_{\mathbf{p}}^{(c)} \mathbf{B}_{\mathbf{p}}^{(c)*}), \quad (2.10)$$

has the standard form.

Taking the Fourier transform of Eq. (2.8) and forming the binary combinations of the fields, one gets the following differential equations:

$$\begin{aligned}\rho'_{\mathbf{q}} &= -\frac{1}{2\sigma_c} \int \frac{d^3k}{(2\pi)^3} k^2 \left[(\mathbf{B}_{\mathbf{k}}^{(c)*} \mathbf{B}_{\mathbf{k}+\mathbf{q}}^{(c)}) + (\mathbf{B}_{\mathbf{k}}^{(c)} \mathbf{B}_{\mathbf{k}-\mathbf{q}}^{(c)*}) \right] \\ &\quad + \frac{1}{2} \int \frac{d^3p}{(2\pi)^3} \frac{d^3k}{(2\pi)^3} p^2 \left[\alpha_{\mathbf{p}-\mathbf{k}}^* \mathbf{A}_{\mathbf{p}}^{(c)} \mathbf{B}_{\mathbf{k}-\mathbf{q}}^{(c)*} + \alpha_{\mathbf{p}-\mathbf{k}} \mathbf{A}_{\mathbf{p}}^{(c)*} \mathbf{B}_{\mathbf{k}+\mathbf{q}}^{(c)} \right], \\ h'_{\mathbf{q}} &= -\frac{1}{\sigma_c} \int \frac{d^3k}{(2\pi)^3} k^2 \left[(\mathbf{A}_{\mathbf{k}}^{(c)*} \mathbf{B}_{\mathbf{k}+\mathbf{q}}^{(c)}) + (\mathbf{A}_{\mathbf{k}-\mathbf{q}}^{(c)*} \mathbf{B}_{\mathbf{k}}^{(c)}) \right] \\ &\quad + \int \frac{d^3p}{(2\pi)^3} \frac{d^3k}{(2\pi)^3} \left\{ \alpha_{\mathbf{p}-\mathbf{k}}^* i (\mathbf{p} \times \mathbf{A}_{\mathbf{k}-\mathbf{q}}^{(c)*}) \mathbf{B}_{\mathbf{p}}^{(c)} \right. \\ &\quad \left. + \alpha_{\mathbf{p}-\mathbf{k}} \frac{1}{k^2} \left[(\mathbf{k}\mathbf{p}) (\mathbf{B}_{\mathbf{p}}^{(c)*} \mathbf{B}_{\mathbf{k}+\mathbf{q}}^{(c)}) - (\mathbf{p}\mathbf{B}_{\mathbf{k}+\mathbf{q}}^{(c)}) (\mathbf{k}\mathbf{B}_{\mathbf{p}}^{(c)*}) \right] \right\},\end{aligned}\quad (2.11)$$

for the spectra $\rho_{\mathbf{p}}(\eta)$ and $h_{\mathbf{p}}(\eta)$ in Eq. (2.9). In Eq. (2.11), $\alpha_{\mathbf{k}} = \int d^3x e^{i\mathbf{k}\mathbf{x}} \alpha(\mathbf{x})$ is the Fourier transform of α -dynamo parameter in Eq. (2.8). We mention that the equations for the spectra in Eq. (2.9) cannot be written in a closed form, analogous to that, e.g., in Refs. [18, 19], for a general coordinate dependent α -dynamo parameter.

3 Axions in the presence of an electromagnetic field

The evolution of an axion field under the influence of an electromagnetic field obeys the following equation in curved spacetime:

$$\frac{1}{\sqrt{-g}} \partial_{\mu} (\sqrt{-g} \partial^{\mu} \varphi) + m^2 \varphi + \frac{g_{a\gamma}}{4} F_{\mu\nu} \tilde{F}^{\mu\nu} = 0, \quad (3.1)$$

where m is the axion mass. Taking the FRW metric and using the conformal variables, We can rewrite Eq. (3.1) in the form,

$$\varphi'' + \frac{2a'}{a} \varphi' - \nabla^2 \varphi + a^2 m^2 \varphi = \frac{g_{a\gamma}}{a^2} (\mathbf{E}_c \mathbf{B}_c), \quad (3.2)$$

where we take the FRW metric and use the conformal variables.

In the Fourier representation, Eq. (3.2) takes the form,

$$\varphi_{\mathbf{k}}'' + \frac{2a'}{a} \varphi_{\mathbf{k}}' + k^2 \varphi_{\mathbf{k}} + a^2 m^2 \varphi_{\mathbf{k}} = \frac{g_{a\gamma}}{a^2} \int \frac{d^3p}{(2\pi)^3} (\mathbf{E}_{\mathbf{p}+\mathbf{k}}^{(c)} \mathbf{B}_{\mathbf{p}}^{(c)*}). \quad (3.3)$$

The integral in the right hand side of Eq. (3.3) differs from the derivative of the magnetic helicity

$$\int \frac{d^3p}{(2\pi)^3} (\mathbf{E}_{\mathbf{p}+\mathbf{k}}^{(c)} \mathbf{B}_{\mathbf{p}}^{(c)*}) \neq -\frac{1}{2} H'(\eta) = \int d^3x (\mathbf{E}_c \mathbf{B}_c) = \int \frac{d^3p}{(2\pi)^3} (\mathbf{E}_{\mathbf{p}}^{(c)} \mathbf{B}_{\mathbf{p}}^{(c)*}), \quad (3.4)$$

which is given in Eq. (2.10).

Nevertheless, we assume that the electromagnetic field is inhomogeneous but isotropic. Thus all odd correlators, like $\langle k_i \rangle$, $\langle k_i k_j k_n \rangle$ etc., vanish. In this case, we rewrite Eq. (3.4) as

$$\int \frac{d^3p}{(2\pi)^3} (\mathbf{E}_{\mathbf{p}+\mathbf{k}}^{(c)} \mathbf{B}_{\mathbf{p}}^{(c)*}) = \int d^3x \exp\left(-\frac{k^2 x^2}{6}\right) (\mathbf{E}_c(\mathbf{x}) \mathbf{B}_c(\mathbf{x})) = -\frac{1}{2} \int \frac{d^3p}{(2\pi)^3} h_{\mathbf{p}}'(\eta) f_{\mathbf{p}}^{(k)*}, \quad (3.5)$$

where $h_{\mathbf{p}}(\eta)$ is the spectrum of the magnetic helicity density in Eq. (2.9) and

$$f_{\mathbf{p}}^{(k)} = \int d^3x e^{i\mathbf{p}\mathbf{x}} \exp\left(-\frac{k^2 x^2}{6}\right) = \frac{6\sqrt{6}\pi^{3/2}}{k^3} \exp\left(-\frac{3p^2}{2k^2}\right). \quad (3.6)$$

is the scalar function.

4 Mean field approximation

Equations (2.11) and (3.3) are difficult to analyze in general case. Thus, we apply the mean field approximation. It implies the consideration of nontrivial spectra which are attributed, however, to the zero mode only.

First, we assume in Eq. (2.11) that $\alpha_{\mathbf{k}} = \alpha_0 \delta^3(\mathbf{k})$, where

$$\alpha_0(\eta) = \int d^3k \alpha_{\mathbf{k}}(\eta) = \frac{4\pi g a \gamma}{\sigma_c} \int k^2 dk \left[\varphi_k'(\eta) + \frac{2k^2}{3\sigma_c} \varphi_k(\eta) \right]. \quad (4.1)$$

In this approximation, we set $\mathbf{q} = 0$ in Eq. (2.11) and consider the mean spectra of the magnetic energy and the magnetic helicity, $\rho(k, \eta) = \frac{k^2}{4\pi^2} (\mathbf{B}_{\mathbf{k}}^{(c)*} \mathbf{B}_{\mathbf{k}}^{(c)})$ and $h(k, \eta) = \frac{k^2}{2\pi^2} (\mathbf{A}_{\mathbf{k}}^{(c)*} \mathbf{B}_{\mathbf{k}}^{(c)})$, which were introduced, e.g., in Refs. [18, 19]. They are related to the total spectra by the expressions,

$$\rho_{\mathbf{q}=0} = \int dk \rho(k, \eta), \quad h_{\mathbf{q}=0} = \int dk h(k, \eta), \quad (4.2)$$

where $\rho_{\mathbf{p}}$ and $h_{\mathbf{p}}$ are given in Eq. (2.9). Using Eq. (2.11) in the considered approximation, we get that the mean spectra obey the equations,

$$\begin{aligned} \frac{\partial \rho(k, \eta)}{\partial \eta} &= -\frac{2k^2}{\sigma_c} \rho(k, \eta) + \alpha_0 k^2 h(k, \eta), \\ \frac{\partial h(k, \eta)}{\partial \eta} &= -\frac{2k^2}{\sigma_c} h(k, \eta) + 4\alpha_0 \rho(k, \eta), \end{aligned} \quad (4.3)$$

which formally coincide with those derived in Refs. [18, 19]. However, Eq. (4.3) involves a nontrivial spectrum of the axion field in Eq. (4.1).

Then, we consider the limit $k \rightarrow 0$ in the integrand in Eq. (3.3). In this case, $f_{\mathbf{p}}^{(k \rightarrow 0)} = (2\pi)^3 \delta^3(\mathbf{p})$ in Eq. (3.6). Using Eq. (3.5) in this approximation and Eq. (4.2), we rewrite Eq. (3.3) in the form,

$$\varphi_k'' + \frac{2a'}{a} \varphi_k' + k^2 \varphi_k + a^2 m^2 \varphi_k = -\frac{g_{a\gamma}}{2a^2} \int dk' \frac{\partial h(k', \eta)}{\partial \eta}, \quad (4.4)$$

which is similar to that used in Ref. [14]. However, we keep the nontrivial spectrum of the axion field in the left hand side.

Equations (4.4) and (4.3), together with Eq. (4.1), form the closed set of the evolution equations, which define the evolution of the magnetic and axion fields. We shall solve them numerically in Secs. 5 and 6.

5 Initial condition and the parameters of the system

We consider the evolution of the system after the QCD phase transition which happens at $T_{\text{QCD}} = 160 \text{ MeV}$. In this situation, the axion mass is taken to be constant, $m = 10^{-6} \text{ eV}$. We use the parameterization in which the scale factor $a = 1/T$ is dimensional, where T is the plasma temperature. The conformal time is defined up to a constant. We take that $\eta = \tilde{M}_{\text{Pl}}(T^{-1} - T_{\text{QCD}}^{-1})$, where $\tilde{M}_{\text{Pl}} = M_{\text{Pl}}/1.66\sqrt{g_*}$, $M_{\text{Pl}} = 1.2 \times 10^{19} \text{ GeV}$ is the Planck mass, and $g_* = 17.25$ is the number of the relativistic degrees of freedom at T_{QCD} [22]. In this case $\eta(T_{\text{QCD}}) = 0$.

We assume that the seed spectrum of the magnetic energy is Kolmogorov, $\rho_0(k) \propto k^n$ with $n = -5/3$. The seed spectrum of the magnetic helicity is $h_0(k) = 2q\rho_0(k)/k$, where $0 \leq q \leq 1$ is the parameter fixing the initial helicity. Note that k is the dimensionless conformal momentum. It spans the range $k_{\text{min}} < k < k_{\text{max}}$, where $k_{\text{min}} = T_{\text{QCD}}/\tilde{M}_{\text{Pl}} = 9.1 \times 10^{-20}$ is the reciprocal horizon size at T_{QCD} . The maximal conformal momentum k_{max} is a free parameter in our model. We take that $k_{\text{max}} < r_{\text{D}}^{-1} = 0.1$, where r_{D} is the conformal Debye radius, to guarantee the plasma electroneutrality.

There is not so much knowledge about the seed axion spectrum. We assume that $\varphi_k^{(0)} = 8\pi^{3/2} f_a \exp(-k^2/\delta^2)/\delta^3$, where δ is the phenomenological parameter. There is the approximate relation between m and f_a [9]: $m = (5.7 \pm 0.007) \mu\text{eV} \left(\frac{10^{12} \text{ GeV}}{f_a} \right)$. Thus, we take $f_a = 10^{12} \text{ GeV}$ since we have chosen $m = 10^{-6} \text{ eV}$. The suggested values of m and f_a are in the sensitivity range of the operating and future lumped element detectors [8] (see also Refs. [20, 21]). We take that $0 \leq k < k_{\text{max}}$ in the axion seed spectrum to be able to probe small momenta. Note that $\varphi_k^{(0)} \rightarrow (2\pi)^3 f_a \delta^3(\mathbf{k})$ at $\delta \rightarrow 0$. In this case, we can reproduce the zero mode approximation studied in Ref. [14]. We shall consider $\delta \sim k_{\text{max}}$ as a rule. Following Ref. [14], we estimate the initial first derivative $\partial_\eta \varphi_k^{(0)}$ basing on the virial theorem. Computing the zero component of the energy-momentum tensor of an axion, we get that $\partial_\eta \varphi_k^{(0)} = \sqrt{k^2 + m^2/T_{\text{QCD}}^2} \varphi_k^{(0)}$.

We introduce the new variables in Eqs. (4.3) and (4.4),

$$\begin{aligned} \rho(k, \eta) &= \frac{R(\kappa, \tau)}{4\pi g_{a\gamma}^2 T_{\text{QCD}}^2 k_{\text{max}}^2}, & h(k, \eta) &= \frac{H(\kappa, \tau)}{2\pi g_{a\gamma}^2 T_{\text{QCD}}^2 k_{\text{max}}^3}, \\ \varphi_k(\eta) &= \frac{\sigma_c}{8\pi g_{a\gamma} k_{\text{max}}^4} \Phi(\kappa, \tau), & \tau &= \frac{2k_{\text{max}}^2}{\sigma_c} \eta, & k &= k_{\text{max}} \kappa, \end{aligned} \quad (5.1)$$

where $0 \leq \tau \leq \tau_{\max} = 2k_{\max}^2 \tilde{M}_{\text{Pl}}/T_{\text{now}}$, $\kappa_m < \kappa < 1$ in the magnetic spectra, whereas $0 < \kappa < 1$ in the axion spectrum, $T_{\text{now}} = 2.7 \text{ K}$ is the current universe temperature, and $\kappa_m = k_{\min}/k_{\max}$. Using Eq. (5.1), Eqs. (4.3) and (4.4) are rewritten in the form,

$$\begin{aligned}
\frac{\partial R}{\partial \tau} &= -\kappa^2 R + \kappa^2 H \int_0^1 \kappa'^2 d\kappa' \left[\frac{\partial \Phi(\kappa', \tau)}{\partial \tau} + \frac{\kappa'^2}{3} \Phi(\kappa', \tau) \right], \\
\frac{\partial H}{\partial \tau} &= -\kappa^2 H + R \int_0^1 \kappa'^2 d\kappa' \left[\frac{\partial \Phi(\kappa', \tau)}{\partial \tau} + \frac{\kappa'^2}{3} \Phi(\kappa', \tau) \right], \\
\frac{\partial^2 \Phi}{\partial \tau^2} &= -\frac{2}{\tilde{a}} \frac{d\tilde{a}}{d\tau} \frac{\partial \Phi}{\partial \tau} - (\kappa^2 \mathcal{K}^2 + \tilde{a}^2 \mu^2) \Phi \\
&\quad + \frac{1}{\tilde{a}^2} \left\{ \int_{\kappa_m}^1 \kappa'^2 H(\kappa', \tau) d\kappa' - \int_{\kappa_m}^1 R(\kappa', \tau) d\kappa' \int_0^1 \kappa'^2 d\kappa' \left[\frac{\partial \Phi(\kappa', \tau)}{\partial \tau} + \frac{\kappa'^2}{3} \Phi(\kappa', \tau) \right] \right\},
\end{aligned} \tag{5.2}$$

where $\mu = \frac{\sigma_c m}{2k_{\max}^2 T_{\text{QCD}}}$ is the effective axion mass, $\mathcal{K} = \sigma_c/2k_{\max}$, $\tilde{a} = 1 + \lambda\tau$, and $\lambda = \frac{\sigma_c T_{\text{QCD}}}{2k_{\max}^2 \tilde{M}_{\text{Pl}}}$.

The initial condition for the new variables in Eq. (5.1) reads

$$R(\kappa, 0) = C\kappa^n, \quad H(\kappa, 0) = q \frac{R(\kappa, 0)}{\kappa}, \quad C = \frac{2\pi g_{a\gamma}^2 T_{\text{QCD}}^2 k_{\max} (n+1) B_c^{(0)2}}{(1 - \kappa_m^{n+1})}, \tag{5.3}$$

where $B_c^{(0)} = B_{\text{now}}/T_{\text{now}}^2 = 3.6 \times 10^{-4}$ is the seed conformal magnetic field which corresponds to present day magnetic field $B_{\text{now}} = 10^{-9} \text{ G}$. Such a strength is within the current constraints on the extragalactic magnetic field obtained in Ref. [23] basing on the cosmic rays observations. However, lower bounds on cosmic magnetic fields are considered in Ref. [24]. The initial condition for the dimensionless axion wavefunction is

$$\begin{aligned}
\Phi(\kappa, 0) &= \frac{32\pi^{3/2} \alpha_{\text{em}} k_{\max}^4}{\sigma_c \delta^3} \exp\left(-\kappa^2 \frac{k_{\max}^2}{\delta^2}\right), \\
\frac{\partial \Phi(\kappa, 0)}{\partial \tau} &= \sqrt{\mathcal{K}^2 \kappa^2 + \mu^2} \Phi(\kappa, 0),
\end{aligned} \tag{5.4}$$

where we take into account that [9] $g_{a\gamma} \approx \frac{\alpha_{\text{em}}}{2\pi f_a}$ and $\alpha_{\text{em}} = 7.3 \times 10^{-3}$ is the fine structure constant.

6 Results

In this section, we show the results of the numerical solution of the system in Eq. (5.2) with the initial condition in Eqs.(5.3) and (5.4).

The system analogous to that in Eq. (5.2) was studied in Ref. [14] for a spatially homogeneous axion. Here, we are mainly focused on the influence of a nontrivial seed spectrum of an axion on the evolution of the system. Thus, we shall probe the behavior of the system for different δ in Eq. (5.4). It is shown in Figs. 1 for $\delta = 5 \times 10^{-11}$ and 2 for $\delta = 10^{-10}$. Unfortunately, we could proceed in numerical simulation only for $T \lesssim T_{\text{QCD}}$ because the system in Eq. (5.2) turned out to be more complicated than that in Ref. [14].

We present the evolution of the magnetic field in Figs. 1(a), 1(b), 2(a), and 2(b). First, we can see that there is no dependence on δ . It generalizes the finding of Refs. [13, 14] for a

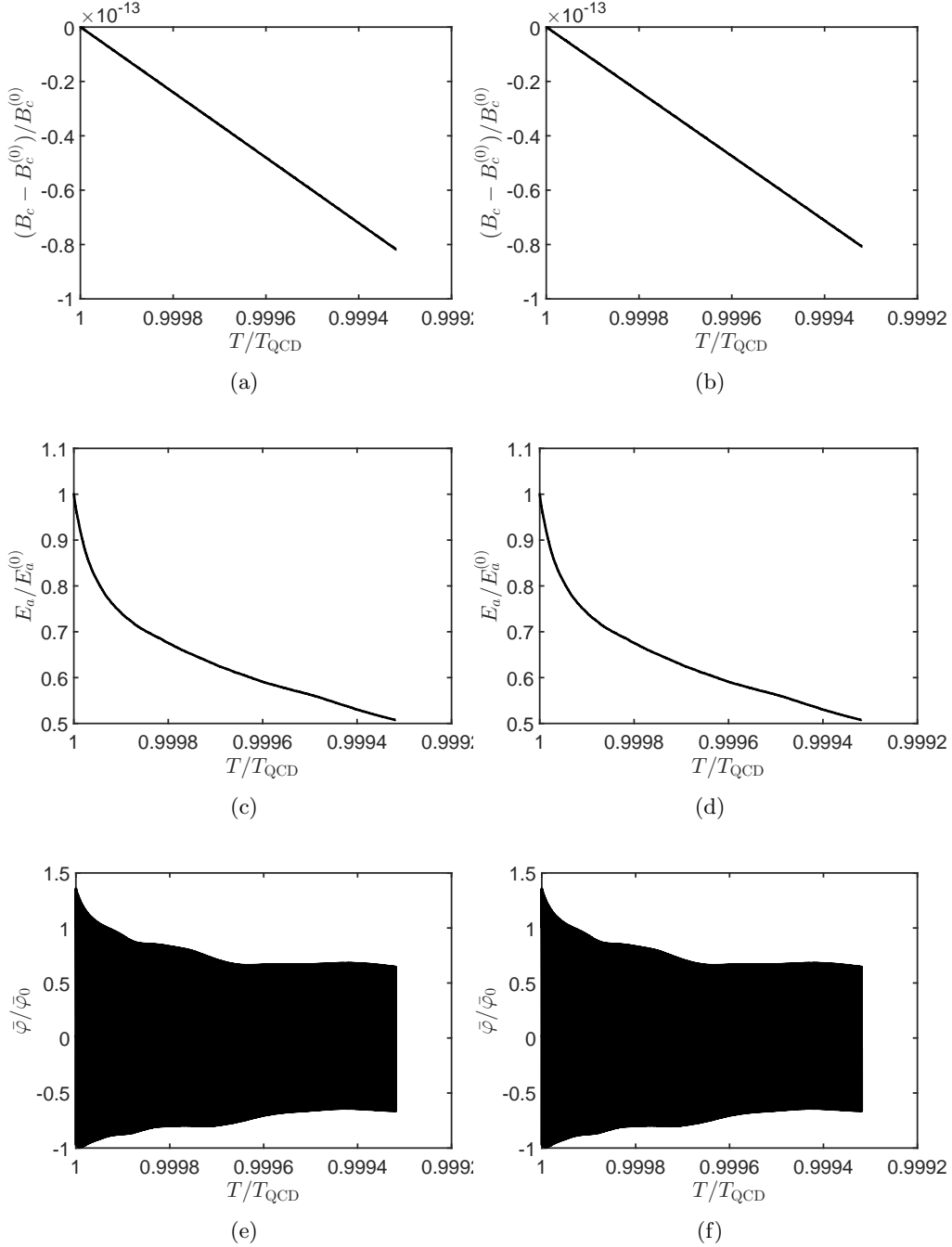


Figure 1: The evolution of the system for the universe cooling down from T_{QCD} . We take that $k_{\text{max}} = 10^{-10}$, $B_c^{(0)} = 3.6 \times 10^{-4}$ ($B_{\text{now}} = 10^{-9}$ G), $m = 10^{-6}$ eV, $f_a = 10^{12}$ GeV, and $\delta = 5 \times 10^{-11}$. Panels (a) and (b): the evolution of the magnetic field. Panels (c) and (d): the behavior of the total axion energy in Eq. (6.1). Panels (e) and (f): the evolution of the averaged axion wavefunction in Eq. (6.2). In panels (a), (c), and (e), we have $q = 1$, whereas in panels (b), (d), and (f) $q = 0$.

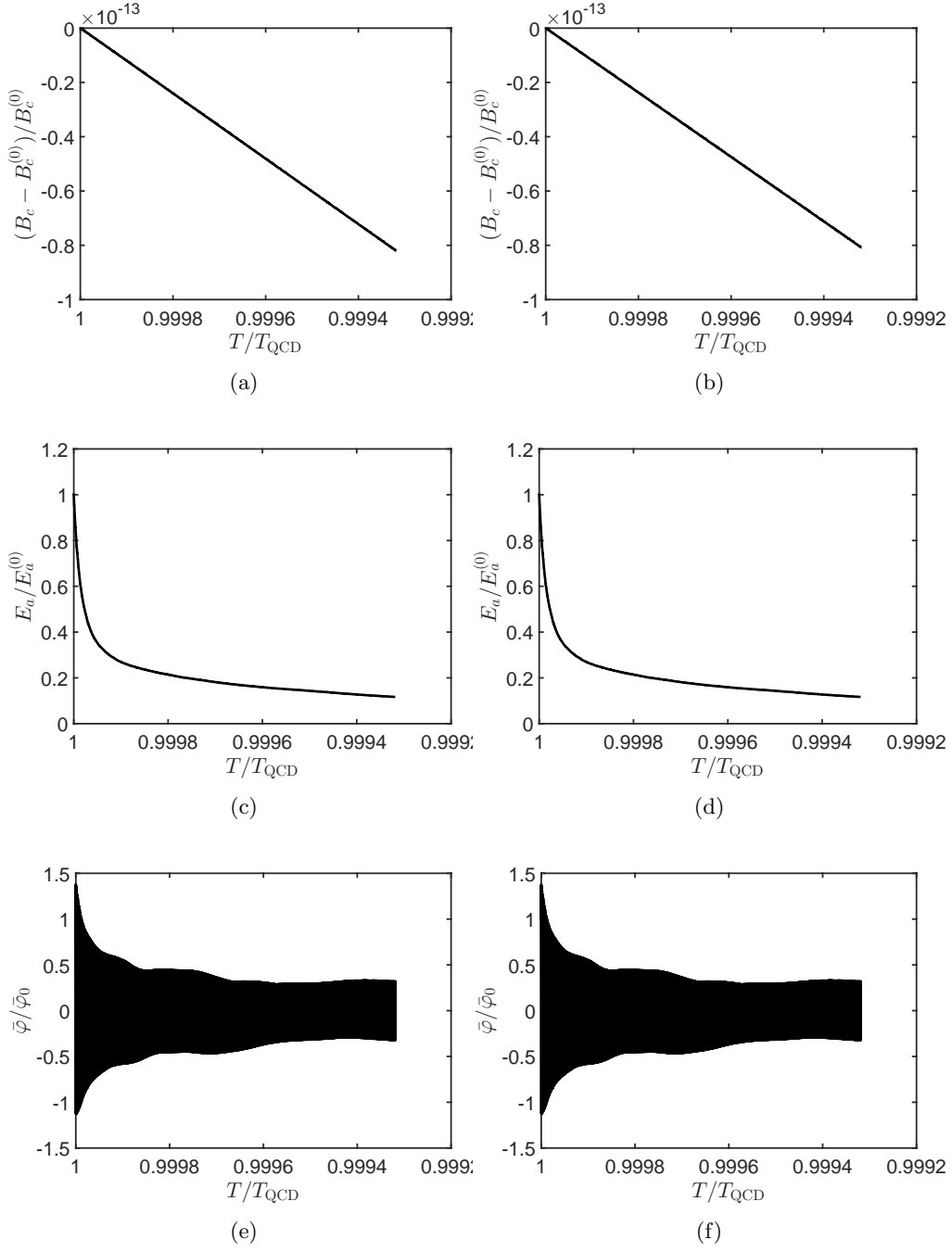


Figure 2: The same as in Fig. 1 for $\delta = 10^{-10}$.

nontrivial seed spectrum of an axion. The slow decay of the magnetic field results from the magnetic diffusion. One has the small dependence of the magnetic field on the seed helicity; cf. Figs. 1(a) and 1(b), as well as Figs. 2(a) and 2(b).

In Figs. 1(c), 1(d), 2(c), and 2(d), we show the total axion energy in the cooling universe, $E_a \propto \int d^3x T_{00}$,

$$E_a = \int_0^1 \kappa^2 d\kappa \left[\left(\frac{\partial \Phi}{\partial \tau} \right)^2 + (\kappa^2 \mathcal{K}^2 + \tilde{a}^2 \mu^2) \Phi^2 \right], \quad (6.1)$$

where T_{00} is the zeroth component of the axion energy-momentum tensor. We normalize E_a on its initial value. Comparing Figs. 2(c) and 2(d) with the results of Ref. [14], we can see that the axion energy decays faster in case of a nontrivial spectrum. Nevertheless, we observe that the smaller δ is, the slower E_a decays. It means that we can reach the agreement with the results of Ref. [14] in the limiting case $\delta \rightarrow 0$, which corresponds to the zero mode approximation. Comparing Figs. 1(c) and 1(d), as well as Figs. 2(c) and 2(d), we can see that the evolution of axions is not affected by the magnetic field at least for the realistic initial conditions used in our simulations. This fact generalizes the finding of Ref. [13, 14] for a nontrivial seed spectrum of axions.

Finally, in Figs. 1(e), 1(f), 2(e), and 2(f), we depict the axion wavefunction averaged over the spectrum,

$$\bar{\varphi}(\eta) = \int_0^{k_{\max}} k^2 dk \varphi_k(\eta), \quad (6.2)$$

which is again normalized on its initial value at T_{QCD} . We can see that it oscillates rapidly. However, unlike Ref. [14], these oscillations are not symmetric with respect to the equilibrium value $\bar{\varphi} = 0$. Surprisingly that the rapid oscillations of $\bar{\varphi}$ are smeared in the total energy in Eq. (6.1) shown in Figs. 1(c), 1(d), 2(c), and 2(d).

We take that $k_{\max} = 10^{-10}$ in our simulations. It means that present length scale obeys $l_{\text{now}} > (k_{\max} T_{\text{now}})^{-1} \approx 10^{-2} R_{\odot}$, where R_{\odot} is the solar radius. Thus the perturbations of the axion field considered in our work, can result in the formation of hypothetical astronomical objects like Bose stars; cf. Ref. [11].

7 Conclusion

In the present work, we have studied the evolution of the system which consists of the axions and magnetic fields. Both axions and magnetic fields are spatially inhomogeneous. The evolution of such a system was considered in the early universe cooling down from the QCD phase transition, with the universe expansion rate being accounted for exactly.

First, in Sec. 2, we have started with the general equations for an electromagnetic field, which interacts with axions, in an arbitrary curved spacetime. Then, taking FRW metric, we have derived the equations for the conformal electric and magnetic fields. Basing on this result, we have obtained the general induction Eq. (2.7) for the magnetic field, which accounts for the spatial distribution of axions. This equation has been further modified to Eq. (2.8) in the isotropic medium. Then, we have obtained the general Eq. (2.11) for the spectra of the magnetic energy and the magnetic helicity.

To describe the evolution of axions in the presence of an electromagnetic field, in Sec. 3, we have considered the general Eq. (3.1) for φ in a curved spacetime. This equation has been rewritten in the Fourier space in Eq. (3.3). An arbitrary magnetic field contributes to the

evolution of axions via the conformal time derivative of the magnetic helicity spectrum in Eq. (3.5).

In order to get the closed system of the evolution equations for a magnetic field and an axion, in Sec. 4, we have applied the mean field approximation which consists in the consideration of the zero mode perturbations. In this situation, we can define the mean spectra, $\rho(k, \eta)$ and $h(k, \eta)$, in Eq. (4.2), as well as derive Eqs. (4.3) and (4.4). Formally, Eqs. (4.3) and (4.4) coincide with those obtained in Ref. [14]. However, they account for the nontrivial spectrum of the α -dynamo parameter.

In Sec. 5, we have chosen the initial conditions and have defined other parameters in Eqs. (4.3) and (4.4). We have considered the evolution of the system below the QCD phase transition when the axion mass takes its vacuum value. It should be noted that there is not so much information about the seed spectrum of axions. We have adopted the initial Gaussian distribution for φ_k which is characterized by the phenomenological parameter δ . One can reproduce, e.g., the zero mode case, discussed in Refs. [13, 14], by setting $\delta \rightarrow 0$. For the magnetic field, we have chosen the seed Kolmogorov spectrum with realistic parameters. Finally, we have rewritten the evolution equations in the form convenient for numerical simulations; cf. Eq. (5.2).

We numerical solution of Eq. (5.2) has been present in Sec. 6. We have been mainly interested in the dependence of the results on the seed axion spectrum. We evolution of the system is shown in Figs. 1 and 2 which correspond to different δ . We have found that the behavior of φ approaches to that described in Ref. [14] while δ decreases. The result of Refs. [13, 14], that there is no mutual influence of magnetic fields and axions, has been confirmed in the case beyond the zero mode approximation. At least, it is valid for the realistic parameters considered in our simulations. The magnetic field turns out to be slowly decreasing. It can be explained by the magnetic diffusion. We have also observed the small dependence of the magnetic field on the seed magnetic helicity.

Acknowledgments

I am thankful to P. M. Akhmetev and S. V. Troitsky for useful discussions.

References

- [1] R. D. Peccei and H. R. Quinn, CP Conservation in the Presence of PseudopartiPeccei and H. R. Quinnclcs, *Phys. Rev. Lett.* 38, 1440–443 (1977).
- [2] C. Abel et al., Measurement of the permanent electric dipole moment of the neutron, *Phys. Rev. Lett.* 124, 081803 (2020) [arXiv:2001.11966].
- [3] L. Di Luzio, M. Giannotti, E. Nardi, and L. Visinelli, The landscape of QCD axion models, *Phys. Rept.* 870, 1–117 (2020) [arXiv:2003.01100].
- [4] P. W. Graham, I. G. Irastorza, S. K. Lamoreaux, A. Lindner, and K. A. van Bibber, Experimental searches for the axion and axion-like particles, *Annu. Rev. Nucl. Part. Sci.* 65, 485–514 (2015) [arXiv:1602.00039].
- [5] E. Aprile et al. (XENON Collaboration), Excess electronic recoil events in XENON1T, *Phys. Rev. D* 102, 072004 (2020) [arXiv:2006.09721].

- [6] V. Anastassopoulos et al. (CAST Collaboration), New CAST limit on the axion-photon interaction, *Nature Phys.* 13, 584–590 (2017) [arXiv:1705.02290].
- [7] M. Buschmann, R. T. Co, C. Dessert, and B. R. Safdi, Axion Emission Can Explain a New Hard X-Ray Excess from Nearby Isolated Neutron Stars, *Phys. Rev. Lett.* 126, 021102 (2021) [arXiv:1910.04164].
- [8] Y. K. Semertzidis and S. Youn, Axion Dark Matter: How to see it?, submitted to *Science Advances* [arXiv:2104.14831].
- [9] F. Chadha-Day, J. Ellis, and D. J. E. Marsh, Axion Dark Matter: What is it and Why Now?, submitted to *Science Advances* [arXiv:2105.01406].
- [10] D. J. E. Marsh, Axion Cosmology, *Phys. Rept.* 643, 1–79 (2016) [arXiv:1510.07633].
- [11] E. W. Kolb and I. I. Tkachev, Axion miniclusters and Bose stars, *Phys. Rev. Lett.* 71, 3051–3054 (1993) [hep-ph/9303313].
- [12] J. Enander, A. Pargner and T. Schwetz, Axion minicluster power spectrum and mass function, *J. Cosmol. Astropart. Phys.* 12 (2017) 038 [arXiv:1708.04466].
- [13] A. Long and T. Vachaspati, Implications of a primordial magnetic field for magnetic monopoles, axions, and Dirac neutrinos, *Phys. Rev. D* 91, 103522 (2015) [arXiv:1504.03319].
- [14] M. Dvornikov and V. B. Semikoz, Evolution of axions in the presence of primordial magnetic fields, *Phys. Rev. D* 102, 123526 (2020) [arXiv:2011.12712].
- [15] K. Fukushima, D. E. Kharzeev, and H. J. Warringa, The chiral magnetic effect. *Phys. Rev. D*, 78, 074033 (2008) [arXiv:0808.3382].
- [16] A. Brandenburg, J. Schober, I. Rogachevskii, T. Kahniashvili, A. Boyarsky, J. Frohlich, O. Ruchayskiy, and N. Kleeorin, The Turbulent Chiral Magnetic Cascade in the Early Universe, *Astrophys. J. Lett.* 845, L21 (2017) [arXiv:1707.03385].
- [17] A. Brandenburg, K. Enqvist, and P. Olesen, Large-scale magnetic fields from hydro-magnetic turbulence in the very early universe, *Phys. Rev. D* 54, 1291 (1996) [astro-ph/9602031].
- [18] A. Boyarsky, J. Frohlich, and O. Ruchayskiy, Self-Consistent Evolution of Magnetic Fields and Chiral Asymmetry in the Early Universe, *Phys. Rev. Lett.* 108, 031301 (2012) [arXiv:1109.3350].
- [19] M. Dvornikov and V. B. Semikoz, Instability of magnetic fields in electroweak plasma driven by neutrino asymmetries, *J. Cosmol. Astropart. Phys.* 05 (2014) 002 [arXiv:1311.5267].
- [20] J. L. Ouellet et al., First Results from ABRACADABRA-10 cm: A Search for Sub- μeV Axion Dark Matter, *Phys. Rev. Lett.* 122, 121802 (2019) [arXiv:1810.12257].
- [21] A. V. Gramolin, D. Aybas, D. Johnson, J. Adam, and A. O. Sushkov, Search for axion-like dark matter with ferromagnets, *Nature Phys.* 17, 79–84 (2021) [arXiv:2003.03348].

- [22] L. Husdal, On Effective Degrees of Freedom in the Early Universe, *Galaxies* 4, 78 (2016) [arXiv:1609.04979].
- [23] A. van Vliet, A. Palladino, A. Taylor, and W. Winter, Extragalactic magnetic field constraints from ultra-high-energy cosmic rays from local galaxies, *Mon. Not. R. Astron. Soc.* 510, 1289–1297 (2022) [arXiv:2104.05732].
- [24] A. Neronov, D. Semikoz, and O. Kalashev, Limit on intergalactic magnetic field from ultra-high-energy cosmic ray hotspot in Perseus-Pisces region [arXiv:2112.08202].